Journal of the European Ceramic Society 18 (1998) 1301–1305

PII: S0955-2219(98)00057-0
0955-2219/98/$—see front matter

Differentiation between Hydroxyapatite and β-Tricalcium Phosphate by Means of μ-Raman Spectroscopy

R. Cuscó,[a]* F. Guitián,[b] S. de Aza[c] and L. Artús[a]

[a]Institut Jaume Almera, Consell Superior d'Investigacions Científiques (CSIC), Lluís Solé i Sabarís s.n., 08028 Barcelona, Spain
[b]Instituto de Cerámica, University of Santiago de Compostela, 15706 Santiago de Compostela, Spain
[c]Instituto de Cerámica y Vidrio, Consejo Superior de Investigaciones Científicas (CSIC), Arganda del Rey, Madrid, Spain

Abstract

We present a comparative study of the Raman spectra of polycrystalline β-tricalcium phosphate (β-TCP) and hydroxyapatite (HA) over their whole optical frequency range. Due to their structural differences, Raman scattering permits to differentiate between these two calcium phosphates, not only through the detection of vibrational modes associated with the OH^- group of hydroxyapatite, but also by comparing the bands arising from internal PO_4^{3-} modes. The widths of the Raman-scattering bands associated with PO_4^{3-} bond-bending modes and the frequency gap between them are characteristic features that can be used to distinguish between β-TCP and HA. The method is used to identify a HA layer a few microns thick which precipitates on the surface of TCP–wollastonite eutectic soaked in simulated body fluid. © *1998 Elsevier Science Limited. All rights reserved*

1 Introduction

Hydroxyapatite (HA) is a calcium phosphate compound which plays a central role in the development of materials for cementless prosthetic implants. Because of its bioactivity properties, HA joins directly to the bone and favours implant fixation, whereas, by contrast, tricalcium phosphate (TCP), another closely related calcium phosphate compound whose stable phase at room temperature is β-TCP, is resorbable.[1,2]

Since during the synthesis of HA variable quantities of β-TCP can be produced depending on pH conditions, Ca/P ratio, ageing time and temperature, the characterization of the final product to check for the presence of β-TCP is of great importance. In fact, the variability of results found in the literature regarding the actual bonding of HA-based implants with bone tissue might be partly due to the presence of a certain amount of β-TCP in the synthetic HA. For other implant materials such as bioglasses it has been recognized that the formation of a HA layer on the surface of the implant[3] is correlated with the bioactivity index of the material. Micro-Raman spectroscopy is a powerful and nondestructive tool that can be used to identify locally different phases present in the material. In particular it can be used to analyse, on a length scale of the order of 1 μm, the chemical and structural changes occurring on the surface of bioactive materials exposed to simulated body fluid (SBF).

2 Experimental

To clearly establish the differences between the Raman spectra of HA and β-TCP, we recorded Raman spectra of pure polycrystalline samples of each coumpound obtained by chemical synthesis. Pure polycrystalline HA was obtained at room temperature by stoichiometric reaction of $Ca(NO_3)_2$ 0·431 M and H_3PO_4 0·258 M solutions at pH 11 in a closed reactor with continuous stirring, leaving the precipitate to age for 1 day, also with continuous stirring. After drying at 110°C for 24 h, the precipitate was isostatically pressed into pellets, which were subsequently heated in air atmosphere in an electric furnace at a rate of 5°C/min up to 800°C. The samples were maintained at this temperature for 1 h, with a water vapour pressure of 10 mm Hg, before being furnace cooled. The Ca/P molar ratio of these samples was determined by ICP-AES and found to be 1·67 ± 0·01. X-ray

*To whom correspondence should be addressed.

diffraction analysis only revealed the presence of the HA phase. Pure polycrystalline β-TCP samples were obtained from $Ca(NO_3)_2$ 0·7 M and H_3PO_4 0·5 M solutions at pH 11 with an initial mixing molar ratio Ca/P = 1·40 in order to avoid the formation of small quantities of HA. The precipitate was dried at 110°C for 24 h and isostatically pressed into pellets. These were heated in an electric furnace at a rate of 5°C/min up to 1000°C, and annealed at this temperature for 1 h. The Ca/P molar ratio of the obtained samples was determined by ICP-AES and was found to be 1·50 ± 0·01. X-ray diffraction analysis of the samples revealed a pure β-TCP phase with no detectable presence of any other calcium phosphate phase.

The calcium phosphate layer that we have characterized by means of μ-Raman spectroscopy was formed on a wollastonite–TCP bioceramic soaked in SBF at 36·5°C for 3 weeks. The wollastonite–TCP bioceramic (Bioeutectic®) was obtained by heating the eutectic composition (60% in weight wollastonite/40% in weight TCP) at 1500°C for 2 h, and by subsequently cooling the melt to 1390°C at a rate of 0·5°C/h.[4] Eutectic microstructures composed of spherical colonies of alternating radial lamellae of wollastonite and TCP were obtained.

The Raman scattering measurements were performed using a Jobin–Yvon T64000 spectrometer equipped with a microscope. The Raman signal was detected by a multichannel CCD detector cooled with liquid nitrogen. The Raman spectra were recorded using the double subtractive configuration of the spectrometer with 100-μm slits. The light was collected in backscattering geometry through an objective of numerical aperture 0·95. The 488-nm line of an Ar^+ laser was used as excitation, focused to a spot of ~1 μm diameter, with an incident power on the sample of ~2 mW.

3 Results and Discussion

The vibrational spectra of both β-TCP[5] and HA[6,7] exhibit a strong molecular character associated with the internal modes of the PO_4^{3-} tetrahedra.[8]

The vibrational normal modes of the free tetrahedron (T_d point group symmetry) are well-known,[9] and give rise to four different frequencies: ν_1, ν_2, ν_3 and ν_4. The ν_1 frequency corresponds to the symmetric stretching of the P–O bonds (A_1 symmetry), whereas the ν_3 frequency arises from the triply degenerate T_2 mode involving asymmetric P–O stretching and also P motion. The ν_2 frequency corresponds to the doubly degenerate O–P–O bending modes (E symmetry), and the ν_4 frequency is due to the triply degenerate T_2 modes of mainly O–P–O bending character. The values of the normal-mode frequencies of the PO_4^{3-} tetrahedron, obtained from Raman scattering measurements on phosphates in aqueous solution, are $\nu_1 = 938\,cm^{-1}$, $\nu_2 = 420\,cm^{-1}$, $\nu_3 = 1017\,cm^{-1}$ and $\nu_4 = 567\,cm^{-1}$.[10] In molecular crystals, such as HA and TCP, the crystalline field induces distortions in the PO_4^{3-} tetrahedra, which change the intratetrahedral bond lengths and angles, and give rise to shifts and splittings of the PO_4^{3-} normal modes. Consequently, the resulting internal PO_4^{3-} bands depend on the crystallographic structure of each compound.

Figure 1 shows the Raman spectrum of HA over its whole optical frequency range. Four Raman-scattering bands, which can be straightforwardly associated with the four normal mode frequencies of the PO_4^{3-} tetrahedron mentioned above, clearly dominate the spectrum. Whereas a single, intense peak arising from the nondegenerate ν_1 mode of the PO_4^{3-} tetrahedron is detected at $962\,cm^{-1}$, several peaks can be observed in the bands originating from the doubly degenerate ν_2 and triply degenerate ν_4 and ν_3 tetrahedron modes, which span a frequency range of 400–490, 570–625 and 1020–1095 cm^{-1}, respectively. These internal PO_4^{3-} bands are centred at frequencies between 20 and 25 cm^{-1} higher than those of the corresponding free-tetrahedron normal modes. In addition to the internal PO_4^{3-} bands, several peaks are detected between 50 and 320 cm^{-1}, which are due to translational modes of the Ca^{2+} and PO_4^{3-} sublattices

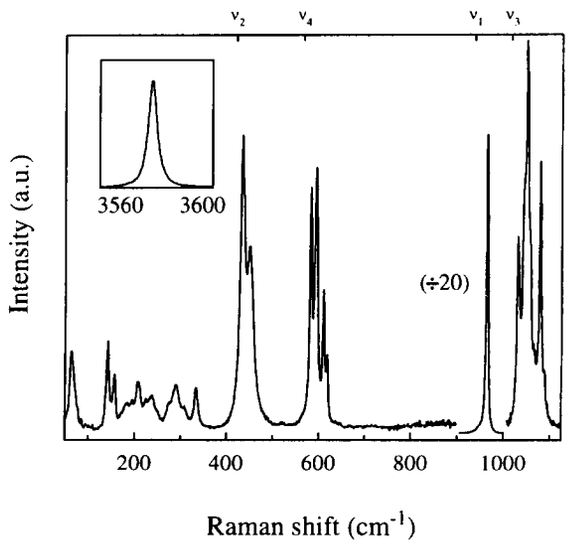

Fig. 1. Raman spectrum of pure polycrystalline HA. The frequencies of the normal modes of the free PO_4^{3-} tetrahedron are indicated by ν_1, ν_2, ν_3 and ν_4 on the top frequency axis. Note the different intensity scale for the ν_1 peak. The spectral region corresponding to the O–H stretching vibrations is shown in the inset. The intensity ratio between the O–H stretching peak at $3576\,cm^{-1}$ and the symmetric stretching peak at $962\,cm^{-1}$ is 0·22.

and rotational modes of the PO_4^{3-} group.[6,11] The bond-stretching mode associated with the OH^- group is also detected as a sharp peak at 3576 cm^{-1}, whereas the translational modes associated with the OH^- sublattice yield a Raman peak at 335 cm^{-1}.[6,7] The fact that the vibrational frequency of the OH^- bond-stretching mode is far from all the internal and external mode frequencies of the calcium phosphate compounds allows one to distinguish unambiguously between HA and TCP when this mode can be detected. However, as we shall see below, the detection of this peak above the background noise is very difficult in samples of a lesser degree of crystallinity. Therefore, to establish the distinction between HA and β-TCP one should look for differential features in the dominant PO_4^{3-} internal bands.

Figure 2 shows the Raman spectrum of β-TCP. As in the case of HA, the spectrum is dominated by the internal PO_4^{3-} bands, which are also centred around frequencies 20–30 cm^{-1} higher than the corresponding normal modes of the PO_4^{3-} tetrahedron, indicating a similarly strong crystalline field in both structures. However, whereas β-TCP crystallizes in the *R*3*c* space group and its unit cell contains 42 PO_4^{3-} tetrahedra,[12] HA crystallizes in the $P6_3/m$ space group and its unit cell contains only six PO_4^{3-} tetrahedra.[13] As discussed in detail in Ref. [7], sizeable differences between the internal PO_4^{3-} modes in HA and β-TCP arise from the highly different degree of complexity of their respective crystalline structures. Since the number of PO_4^{3-} tetrahedra in the unit cell is seven times larger for β-TCP than for HA, a correspondingly larger number of internal modes, whose frequencies will be slightly shifted due to correlation

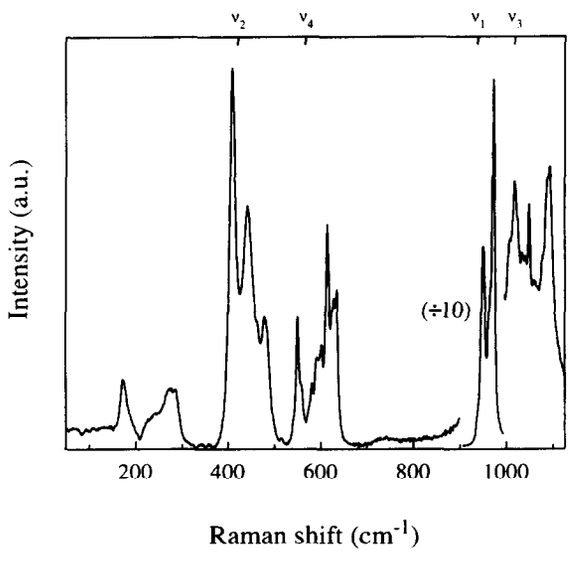

Fig. 2. Raman spectrum of pure polycrystalline β-TCP. The frequencies of the normal modes of the free PO_4^{3-} tetrahedron are indicated by ν_1, ν_2, ν_3 and ν_4 on the top frequency axis. Note the different intensity scale for the ν_1 band.

effects, is expected in β-TCP. Furthermore, whereas the six PO_4^{3-} tetrahedra in the HA unit cell are crystallographically equivalent, three nonequivalent types of tetrahedra can be distinguished in the β-TCP unit cell.[12] As a consequence of the differences in intratetrahedral bond lengths and angles, the spread of frequencies of the split PO_4^{3-} modes is significantly larger for β-TCP. The effects of tetrahedra distortions on the frequency regions spanned by the internal PO_4^{3-} bands have been described by an elastic model, which reproduces the trends observed in the Raman spectra taking into account the changes in the force constants due to variations in bond lengths.[7] The effects of the existence of three nonequivalent tetrahedra which are differently distorted can be clearly observed in the internal band arising from the nondegenerate ν_1 symmetric stretching mode of the tetrahedron. Whereas a single intense peak at $\nu = 962\ cm^{-1}$ is detected in HA, two peaks and a shoulder can be observed in β-TCP. The Raman spectra of β-TCP and HA also exhibit clear differences in the asymmetric stretching and O–P–O bond-bending regions. The bands arising from the doubly degenerate ν_2 and triply degenerate ν_4 modes, although being centred around the same frequencies, span a different frequency range in HA and β-TCP. Thus, for β-TCP we find ν_2 modes in the 370–505 cm^{-1} range and ν_4 modes in the 530–645 cm^{-1}. Therefore, whereas Raman scattering bands arising from ν_2 and ν_4 modes are separated by a frequency gap of ~120 cm^{-1} in HA, the gap is of only ~55 cm^{-1} in β-TCP. This is a characteristic spectral feature, which can be used to distinguish between HA and β-TCP even in samples with poor crystallinity where the resolution of individual peaks in these bands as well as the detection of the O–H stretching mode of HA can be difficult. In samples with a high degree of cystallinity there are also noticeable differences at frequencies below the ν_2 band, in the lattice-mode region corresponding to Ca^{2+} and PO_4^{3-} translational modes, and PO_4^{3-} librational modes. Whereas several sharp peaks are resolved in HA, only a broad peak and a featureless band is observed in β-TCP. This is also related to the much more complex crystal structure of β-TCP, in which cation sites with partial occupancy and positional disorder of certain PO_4^{3-} groups are present.[12]

Once the Raman spectra of pure, polycrystalline reference specimens of HA and β-TCP have been characterized, μ-Raman spectroscopy can be used to distinguish between these two compounds in the calcium phosphate layers which precipitate on the surface of bioceramic materials as a result of ionic interchange with SBF. In particular, we use this technique to check that the layer of a few microns

that precipitates on the surface of a wollastonite–TCP bioceramic soaked in SBF for several weeks is composed of HA microcrystals. In Fig. 3 we show the Raman spectrum obtained from the surface layer of the wollastonite–TCP sample described in Section 2. In the frequency range up to 1100 cm^{-1}, only the Raman scattering bands associated with the internal modes of the PO_4^{3-} tetrahedra are detected. In the ν_1 region, an intense single peak is observed at 962 cm^{-1} which, according to the previous discussion, suggests that formation of HA crystals may have taken place. However, the ν_1 peak is noticeably broader in relation to the ν_1 peak of the reference HA spectrum shown in Fig. 1. Therefore, the possibility that this peak might contain the unresolved ν_1 peaks of β-TCP (see Fig. 2) cannot be ruled out from the onset. The fact that the ν_1 peak is broader for the HA layer precipitated on wollastonite–TCP than for the reference HA sample reflects the poorer crystallinity of the former. This is not surprising considering that the precipitation conditions of synthetic HA were optimized and that the sample was subsequently heated up to 800°C to improve its crystallinity. Thus, the differences between the bond-bending internal bands of HA and β-TCP may provide a more useful criterion to discern between these two calcium phosphates in poor crystallinity samples. To confirm the identification of HA, we observe from Fig. 3 that the bands corresponding to the ν_2 and ν_4 bond-bending modes of the tetrahedra are relatively narrow and well-separated. The widths of these bands are 47 cm^{-1} for the ν_2 band and 50 cm^{-1} for the ν_4 band. These values are in better agreement with the widths found for the HA reference sample than with those of β-TCP. Furthermore, the separation between these two bands is found to be about 110 cm^{-1}, a value close to that of ~120 cm^{-1} found for the HA reference spectrum of Fig. 1 and clearly inconsistent with the band separation of 55 cm^{-1} found in the β-TCP reference spectrum. To further support the identification of the surface layer as HA we recorded the spectrum in the O–H stretching-mode region, which is shown in the inset of Fig. 3. A very weak signal detected around 3580 cm^{-1} confirms the presence of the OH^- group in the structure. Therefore, we conclude that HA crystals have been formed on the wollastonite-TCP bioceramic after being soaked in SBF under the conditions reported in Section 2.

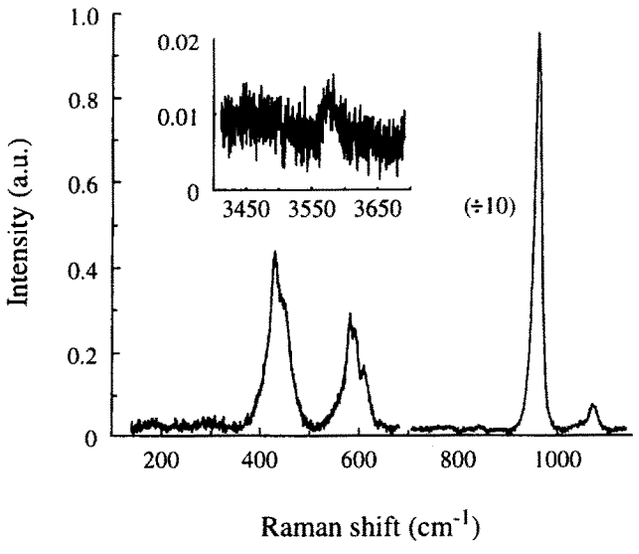

Fig. 3. Raman spectrum obtained from the surface region of a cross section of a wollastonite–TCP bioceramic soaked in SBF. Comparison with the spectrum of Fig. 1 allows us to identify this calcium phosphate layer as HA. The O–H bond stretching region of the spectra is shown in the inset. Note the different intensity scales.

4 Conclusions

We have presented a comparative study of the Raman spectra of synthetic HA and β-TCP aimed at providing suitable criteria to differenciate between these two calcium phosphate compounds with highly different bioactivity behaviour. We have shown that, apart from the modes associated with the OH^- group of HA, which are usually difficult to detect in samples with poor crystallinity, and the different number of ν_1 peaks detected in each compound, the ν_2 and ν_4 bending modes exhibit noticeable differences which can be used to discern between HA and β-TCP. In particular, the frequency gap between the bands arising from the ν_2 and ν_4 bond-bending modes of the PO_4^{3-} tetrahedra can be used as a fingerprint to distinguish between these two calcium phosphates. Therefore, Raman spectroscopy has proven to be a powerful nondestructive technique to distinguish between HA and β-TCP crystals. Finally, it has been shown by means of μ-Raman spectroscopy that HA crystals are formed on the surface of wollastonite–TCP bioceramics soaked in SBF.

References

1. Hench, L. L. and Clark, A. E., Adhesion to bone. In *Biocompatibility of Orthopaedic Implants*, Vol. 2, Chapter 6, ed. D. F. Williams. CRC Press, Boca Raton, FL, 1982.
2. Hench, L. L., Bioactive ceramics. In *Bioceramics: Materials Characteristic Versus In Vivo Behaviour*, ed. P. Ducheyne and J. Lemons. Annals NY Acad. Sci., Vol. 523, 1988, p. 54.
3. Kim, C. Y., Clark, A. E. and Hench, L. L., Early stages of calcium phosphate layer formation in Bioglass. *J. Non-Crystalline Solids*, 1989, **113**, 195–202.
4. P. N. de Aza, Biomateriales de Wollastonita y de Sistemas Binarios conteniendo Wollastonita. Ph.D. thesis,

University of Santiago de Compostela, La Coruña, Spain, 1995.

5. de Aza, P. N., Santos, C., Pazo, A., de Aza, S., Cuscó, R. and Artús, L., Vibrational properties of calcium phosphate compounds. I. Raman spectrum of β-tricalcium phosphate. *Chem. Mater.*, 1997, **9**, 912–915.
6. Iqbal, Z., Tomaselli, V. P., Fahrenfeld, O., Möller, K. D., Ruszala, F.A. and Kostiner, E., Polarized Raman scattering and low frequency infrared study of hydroxyapatite. *J. Phys. Chem. Solids*, 1977, **38**, 923–927.
7. de Aza, P. N., Guitián, F., Santos, C., de Aza, S., Cuscó, R. and Artús, L., Vibrational properties of calcium phosphate compounds. II. Comparison between hydroxyapatite and β-tricalcium phosphate. *Chem. Mater.*, 1997, **9**, 916–922.
8. Kravitz, L. C., Kingsley, J. D. and Elkin, E. L., Raman and infrared studies of coupled PO_4^{3-} vibrations. *J. Chem. Phys.*, 1968, **49**, 4600–4610.
9. Herzberg, G., *Molecular Spectra and Molecular Structure II. Infra-Red and Raman Spectra of Polyatomic Molecules*. D. Van Nostrand, Princeton, 1945.
10. Nakamoto, K., *Infrared and Raman Spectra of Inorganic Coordination Compounds*. John Wiley and Sons, New York, 1986, p. 138.
11. Fowler, B. O., Infrared Studies of Apatites. I. Vibrational assignments for calcium, strontium, and barium hydroxyapatites utilizing isotopic substitution. *Inorganic Chemistry*, 1973, **13**, 194–207.
12. Dickens, B., Schroeder, L. W. and Brown, W. E., Crystallographic studies of the role of Mg as a stabilizing impurity in β-$Ca_3(PO_4)_2$. I. The crystal structure of pure β-$Ca_3(PO4)_2$. *J. Sol. Stat. Chem.*, 1974, **10**(PO4), 232–248.
13. Kay, M. I., Young, R. A. and Posner, A. S., Crystal structure of hydroxyapatite. *Nature*, 1964, **204**, 1050–1052.